

## Full Length Article

Correlation between  $^{18}\text{F}$ -Sodium Fluoride positron emission tomography and bone histomorphometry in dialysis patients

Louise Aaltonen<sup>a,\*</sup>, Niina Koivuviita<sup>a</sup>, Marko Seppänen<sup>b</sup>, Xiaoyu Tong<sup>c</sup>, Heikki Kröger<sup>c,d</sup>, Eliisa Löyttyniemi<sup>e</sup>, Kaj Metsärinne<sup>a</sup>

<sup>a</sup> Kidney Center, Department of Medicine, Turku University Hospital, PL 52, Kiinamylynkatu 4-8, Turku 20521, Finland

<sup>b</sup> Department of Clinical Physiology, Nuclear Medicine and Turku PET Centre, University of Turku, Kiinamylynkatu 4-8, Turku 20521, Finland

<sup>c</sup> Kuopio Musculoskeletal Research Unit (KMRU), Institute of Clinical Medicine, University of Eastern Finland, POB 1627, Kuopio, Finland

<sup>d</sup> Kuopio University Hospital, Kuopio, Finland

<sup>e</sup> Department of Biostatistics, University of Turku, Kiinamylynkatu 10, 20014 Turku, Finland

## ARTICLE INFO

## Keywords:

$^{18}\text{F}$ -NaF PET

Bone biopsy

Bone histomorphometry

Renal osteodystrophy

## ABSTRACT

**Background:** The diagnosis of renal osteodystrophy is challenging. Bone biopsy is the gold standard, but it is invasive and limited to one site of the skeleton. The ability of biomarkers to estimate the underlying bone pathology is limited.  $^{18}\text{F}$ -Sodium Fluoride positron emission tomography ( $^{18}\text{F}$ -NaF PET) is a noninvasive quantitative imaging technique that allows assessment of regional bone turnover at clinically relevant sites. The hypothesis of this study was, that  $^{18}\text{F}$ -NaF PET correlates with bone histomorphometry in dialysis patients and could act as a noninvasive diagnostic tool in this patient group.

**Methods:** This was a cross-sectional diagnostic test study. 26 dialysis patients with biochemical abnormalities indicating mineral and bone disorder were included. All the participants underwent a  $^{18}\text{F}$ -NaF PET scan and a bone biopsy. Fluoride activity in the PET scan was measured in the lumbar spine and at the anterior iliac crest. Dynamic and static histomorphometric parameters of the bone biopsy were assessed. As histomorphometric markers for bone turnover we used bone formation rate per bone surface (BFR/BS) and activation frequency per year (Ac.f).

**Results:** There was a statistically significant correlation between fluoride activity in the  $^{18}\text{F}$ -NaF PET scan and histomorphometric parameters such as bone formation rate, activation frequency and osteoclast and osteoblast surfaces and mineralized surfaces.  $^{18}\text{F}$ -NaF PET's sensitivity to recognize low turnover in respect to non-low turnover was 76% and specificity 78%. Because of the small number of patients with high turnover, we were unable to demonstrate significant predictive value in this group.

**Conclusions:** A clear correlation between histomorphometric parameters and fluoride activity in the  $^{18}\text{F}$ -NaF PET scan was established.  $^{18}\text{F}$ -NaF PET may possibly be a noninvasive diagnostic tool in dialysis patients with low turnover bone disease, but further research is needed.

## 1. Introduction

As chronic kidney disease (CKD) progress, abnormalities in mineral homeostasis occur impairing bone remodeling and mineralization [1–3]. Bone abnormalities are found in the majority of patients with CKD stages 3 – 5D [1,4–6]. A high incidence of fractures has been reported in patients with abnormal bone turnover [7,8] and fractures are associated with increased mortality [9]. High and low bone turnover are also associated with vascular calcification and cardiovascular morbidity and mortality [10–12].

The diagnosis of mineral bone disorder and the underlying bone

histology in CKD patients is challenging. The treatment of renal osteodystrophy (ROD) and especially the treatment of fractures in this patient group, depends on the underlying bone histopathology and bone turnover. The gold standard for diagnosing the subtypes of ROD is bone biopsy [1,13,14], but it is invasive, limited to one site of the skeleton and requires considerable expertise regarding quantitative histomorphometry and interpretation [15]. Plasma parathormone (PTH) measurement is commonly used to evaluate these patients, and generally extremely high or low PTH levels predict the underlying bone disorder [16,17]. Still PTHs ability to correctly estimate turnover in bone is limited [18,19], as guidelines recommend PTH range of 2–9

\* Corresponding author at: Kiinamylynkatu 4-8, 20521 Turku, Finland.

E-mail address: [louise.aaltonen@tyks.fi](mailto:louise.aaltonen@tyks.fi) (L. Aaltonen).

<https://doi.org/10.1016/j.bone.2020.115267>

Received 23 October 2019; Received in revised form 3 February 2020; Accepted 9 February 2020

Available online 11 February 2020

8756-3282/ © 2020 The Authors. Published by Elsevier Inc. This is an open access article under the CC BY-NC-ND license

(<http://creativecommons.org/licenses/by-nc-nd/4.0/>).

times normal values in dialysis patients [1]. Total serum alkaline phosphatase does not substantially improve diagnostic accuracy [20]. A recent study showed that biomarkers such as tartrate-resistant acid phosphatase 5b (TRAP5b) and procollagen type 1 N-terminal propeptide (PINP) can discriminate low from non-low turnover better than PTH [21]. However, no biomarker in clinical use has yet been proven suitable or superior to PTH to estimate overall bone histology.

$^{18}\text{F}$ -NaF positron emission tomography ( $^{18}\text{F}$ -NaF PET) is a non-invasive quantitative imaging technique that allows assessment of regional bone turnover at clinically relevant sites [22–24].  $^{18}\text{F}$ -NaF is a bone-seeking tracer, which reflects remodeling of bone and osteoblast activity [25].  $^{18}\text{F}$ -NaF serves as an efficient tracer to measure metabolic changes in bone. Quantitative PET imaging enables measurement of fluoride activity in the bone. The net influx rate of  $^{18}\text{F}$ -Fluoride into bone in the dynamic PET scan is referred to as  $K_i$  and the fractional uptake of  $^{18}\text{F}$ -Fluoride in the static PET scan as FUR. A correlation between histomorphometric markers such as bone formation rate (BFR) and  $K_i$  in  $^{18}\text{F}$ -NaF PET scan in CKD patients has previously been shown in one small study [26].  $^{18}\text{F}$ -NaF PET has also been used to investigate regional bone formation in patients with osteoporosis and Paget's disease [27,28] and also to quantify effects of pharmacological treatments [29].

The aim of our study was to assess the possible correlation between  $^{18}\text{F}$ -NaF PET and bone histomorphometry in dialysis patients. In addition, we wanted to evaluate if  $^{18}\text{F}$ -NaF PET can distinguish between high and low turnover mineral bone disorder. Our hypothesis was that  $^{18}\text{F}$ -NaF PET correlates with histomorphometric parameters in the bone biopsy and could act as a noninvasive diagnostic tool.

## 2. Materials and methods

The study was approved by the Ethics committee of the Hospital District of South Western Finland and was conducted in accordance with Declaration of Helsinki as revised 1966. The study is registered in [ClinicalTrials.gov](https://www.clinicaltrials.gov) protocol registration and result system. All subjects gave written informed consent.

### 2.1. Study subjects

After consenting, 26 patients with end-stage renal disease on dialysis were enrolled. Inclusion criteria were as follows: dialysis vintage for at least 3 months and biochemical abnormalities indicating mineral and bone disorder; long-term elevated PTH-levels and hyperphosphatemia. Exclusion criteria were: pregnancy, previous parathyroidectomy and bisphosphonate medication treatment in the past 6 months.

Ongoing medication for secondary hyperparathyroidism such as phosphate binders, vitamin D or its active metabolites and calcimimetics was continued. During the study period, the medication remained unchanged. All patients were referred to a  $^{18}\text{F}$ -NaF PET scan. A bone biopsy was performed 4–6 weeks after the PET scan, following a standardized tetracycline labeling period. Biochemical markers in clinical use were obtained during this period. Also dual-energy X-ray absorptiometry (DXA) was performed.

In addition, 7 healthy subjects were recruited as a validation group for the PET-imaging. The healthy subjects underwent a  $^{18}\text{F}$ -NaF PET scan after assessment of routine laboratory tests to rule out underlying kidney or bone disease. No bone biopsy was performed.

### 2.2. Laboratory assessment

Serum ionized calcium, alkaline phosphatase, phosphate, 25-hydroxyvitamin D, 1,25-dihydroxyvitamin D, intact parathormone, albumin, acid-base balance, full blood count and creatinine were performed in all patients. Coagulation screen was obtained previous to the bone biopsy. All tests were performed and analyzed by the local

University Hospital laboratory.

### 2.3. Bone biopsy and histomorphometry

Iliac crest biopsies were performed vertically under local anesthesia including one cortex. All patients underwent fluorochrome double labeling by receiving 500 mg tetracycline per os three times daily for two days, followed by a drug free interval of ten days and a further two days administration of tetracycline. Bone biopsy was completed 7–10 days after the second label. Bone biopsies were obtained using a Snarecoil Mermaid Medical RBN-86 8Gx15cm needle. All the patients underwent a successful bone biopsy procedure without complications.

Bone biopsies were fixed in 70% ethanol for at least 48 h before embedding in polymethylmethacrylate. The samples were cut into 5- $\mu\text{m}$  thick sections and then stained with modified Masson-Goldner trichrome stain for static parameters, unstained sections were used for dynamic parameters. A semiautomatic image analyzer (BioquantOsteoII, Bioquant Image Analysis Corporation, Nashville, TN, USA) was used for analyzing of all parameters.

As histomorphometric parameters for bone turnover we used bone formation rate per bone surface (BFR/BS) and activation frequency per year (Ac.f). In 2 patients, there were single tetracycline labels only or the labels were very close to each other and therefore mineral apposition rate (MAR) could not be calculated. In those patients, we used a value for MAR of 0.3  $\mu\text{m}/\text{day}$  in line with American Society for Bone and Mineral Research (ASBMR) Histomorphometry Nomenclature Committee recommendations for biopsies with only single labels [15]. The diagnosis of bone histomorphometry was determined based on turnover-mineralization-volume (TMV) classification for bone histomorphometry [30]. Bone turnover was classified as normal when Ac.f was between 0.49 and 0.72/year and/or BFR/BS was 1.80 to 3.80  $\text{mm}^3/\text{cm}^2$  per year [5]. Bone volume/tissue volume (BV/TV) was considered low when it was below 16.8%. All samples were analyzed by an experienced independent histomorphometrist, who was blinded to the PET results.

### 2.4. $^{18}\text{F}$ -Sodium Fluoride positron emission tomography

The PET scans were acquired using a Discovery VCT scanner (GE Healthcare). The radionuclide,  $^{18}\text{F}$ -Fluoride ( $^{18}\text{F}\text{F}^-$ ) is produced by 11-MeV proton irradiation of  $^{18}\text{O}$ -water using a cyclotron. The quality control tests for the  $^{18}\text{F}$ -NaF are conforming to the European Pharmacopeia. The subjects were positioned supine with the lumbar vertebrae in the field of view. A 60 minute scan of the lumbar spine (L1–L4) followed by a 10 minute static scan of the pelvis was done. The 60 minute dynamic scan was begun simultaneously with an intravenous injection of 200 MBq  $^{18}\text{F}$ -NaF. The dynamic scan consisted of twenty-four 5-second, four 30-second and fourteen 240-second time frames. Low-dose CT-scans were done for image segmentation and attenuation correction. To generate bone activity curves (kilobecquerels per milliliter), regions of interest (ROI) in the lumbar spine were defined by drawing a ROI within each vertebral body, avoiding the end-plates and disk space. In the static PET-scan of the pelvis ROI was defined by drawing a ROI on the anterior iliac crest, in the same region the bone biopsy was later obtained, see Fig. 1. Values were calculated both from the right and the left anterior iliac crest and the mean value was calculated. It is necessary to measure the arterial input function in order to calculate the plasma clearance of fluoride to bone. We used an image derived input function by placing a ROI over the abdominal aorta [31,32]. Patlak analysis was used to estimate the plasma clearance of  $^{18}\text{F}$ -Fluoride (net influx rate,  $K_i$ ) into the bone at the lumbar spine [33]. Patlak analysis cannot be used when analyzing the static scans of the pelvic bone; instead, fractional uptake rate (FUR), which is an approximation of Patlak  $K_i$  [34], was calculated by dividing the bone activity concentration by area-under-curve of blood activity from  $^{18}\text{F}$ -Fluoride administration time to the time of static scan. Activity

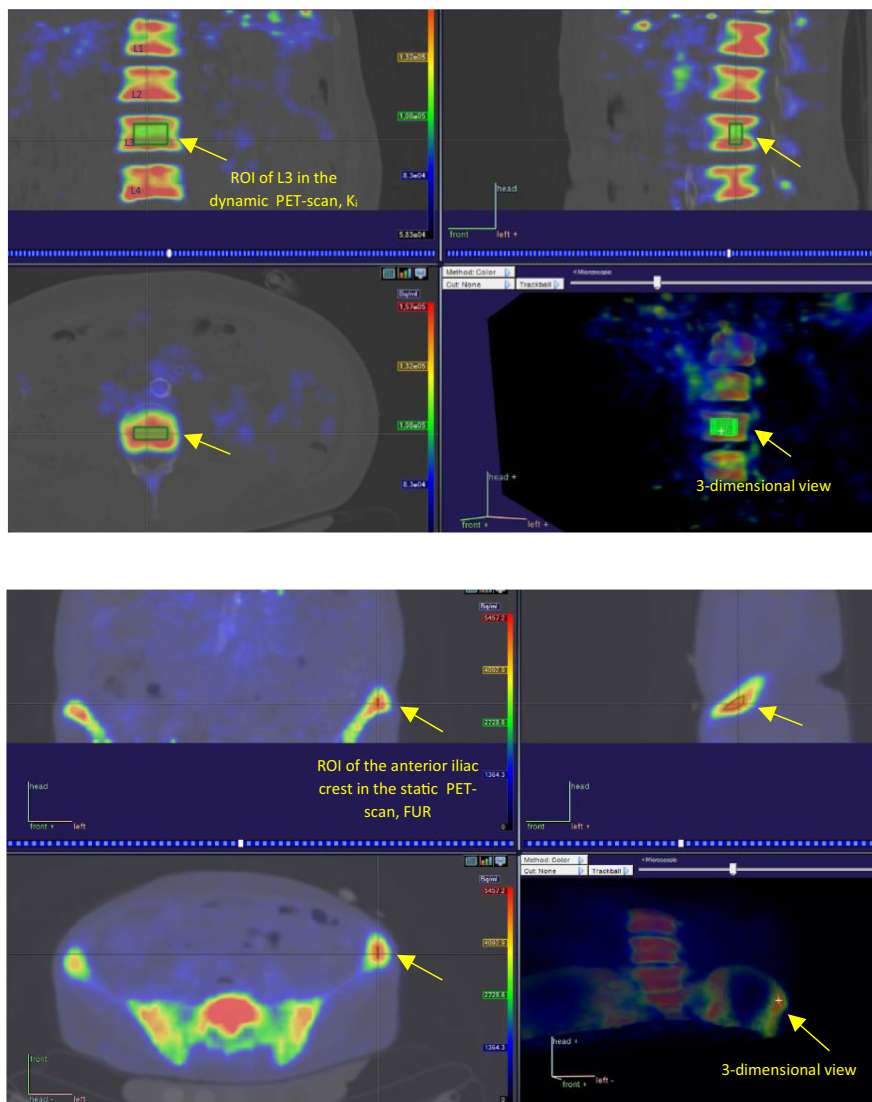


Fig. 1. Regions of interest (ROI) in the dynamic and static PET scan.

measurements were corrected for radioactive decay to the time of injection. In many previous  $^{18}\text{F}$ -NaF PET-studies, standardized uptake value (SUV) is used to estimate the plasma clearance of  $^{18}\text{F}$ -Fluoride. FUR is an approximation of Patlak  $K_i$  [34] and  $K_i$  is more precise and better when assessing treatment response [33].

## 2.5. Statistical analysis

Statistical analyses for background variables were performed using SAS 9.4 for Windows and JMP Pro 13. Normality tests for bone histomorphometric and  $^{18}\text{F}$ -NaF PET was done visually together with the Shapiro-Wilk test. Many of the parameters failed the normality test and therefore nonparametric statistical tests were used. Correlations between bone turnover parameters and fluoride activity in the PET-scan were assessed using the Spearman rank correlation test. Characteristics of the study population were expressed as median and interquartile range (IQR) or mean and standard deviation (SD). For estimating the difference between means in different groups we used one-way analysis of variance (ANOVA) after logarithm transformation. Histomorphometric markers and fluoride activity in the PET-scan were compared based on turnover using Wilcoxon test. We assessed the receiver operating characteristics (ROC) curve for log transformed data. Based on the ROC curve we obtained the area under the curve (AUC)

and calculated sensitivity, specificity and positive and negative predictive values. AUC of 0.6–0.7 was considered as poor, 0.7–0.8 as fair, 0.8–0.9 as good and 0.9–1 as excellent. A p value of 0.05 (two-tailed) or less was considered statistically significant.

## 3. Results

### 3.1. General

The patient demographics and disease characteristics are presented in Table 1. All patients were white, the average age was 68 years. Average dialysis vintage was 12 months and 50% were on peritoneal dialysis. 50% were female. A third had a history of diabetes and 24% were smokers. 65% of the patients were on kidney transplant waiting list and 8% had a history of kidney transplant. 23% had osteoporosis based on the bone biopsy. Based on DXA, 38% of the patients had low bone mineral density. Cause of ESRD, distribution of turnover based on the bone biopsy and medication are also shown in Table 1. Of 30 eligible patients, 3 were excluded because of insufficient bone biopsy and one because of problems with data transmission of the PET-imaging. The flow diagram of the patients is shown in Fig. 2.

**Table 1**  
Characteristics of the study group.

No. of patients	26
Female sex (%)	13 (50)
Age, y (median, range)	68 (37–83)
BMI (mean, SD)	24.2 ± 3.8
Smoker (%)	6 (24)
History of diabetes (%)	10 (40)
fS-calcium-ion mmol/l (median, IQR)	1.18 (1.12–1.24)
fP-phosphorus mmol/l (median, IQR)	1.56 (1.30–1.94)
fP-PTH, ng/ml (median, IQR)	285 (177–496)
P-D-25 nmol/l (median, IQR)	70 (47–88)
S-D-1,25 pmol/l (median, IQR)	30 (24–50)
P-tALP U/l (median, IQR)	84 (60–127)
P-Alb g/l (median, IQR)	30.7 (27.0–33.6)
Turnover based on histomorphometry	
High turnover (%)	3 (12)
Low turnover (%)	17 (65)
Normal turnover (%)	6 (23)
Osteoporosis (bone biopsy) (%)	6 (23)
Dialysis vintage, month (median, range)	12 (4–94)
Dialysis modality PD/HD %	50/50
Cause of ESRD	
Hypertension (%)	3 (12)
Glomerulonephritis (%)	5 (19)
Diabetic nephropathy (%)	9 (34)
Polycystic kidney disease (%)	6 (23)
Other/unknown (%)	3 (12)
On kidney transplantation waiting list (%)	17 (65)
History of kidney transplantation (%)	2 (8)
Medication	
Calcimimetic (%)	3 (12)
Alfacalcidol, Paricalcitol (%)	17 (65)
Calcium carbonate (%)	23 (88)
Calcitriol (%)	25 (96)
Sevelamer/lantane carbonate (%)	16 (62)
Corticosteroid (%)	1 (4)

### 3.2. Histomorphometric findings

On the basis of bone formation rate per bone surface (BFR/BS) and activation frequency (Ac.f), only 12% had high turnover, 65% had low turnover and 23% had normal turnover. Bone histomorphometric parameters of the study group according to turnover are shown in Table 2. Patients with low turnover were in average older than patients with normal or high turnover.

### 3.3. PET-studies

#### 3.3.1. Correlation between $^{18}\text{F}$ -NaF PET and Histomorphometry

Measurements of  $^{18}\text{F}$ fluoride activity in the  $^{18}\text{F}$ -NaF PET in the lumbar region ( $K_i$  mean) and at the anterior iliac crest ( $\text{FUR}_{\text{mean}}$ ) were directly compared to histomorphometric and laboratory parameters using the Spearman rank correlation test. There was a statistically significant correlation between  $K_i$  mean and  $\text{FUR}_{\text{mean}}$  levels and a majority of the histomorphometric parameters, such as bone formation rate (BFR/BS), activation frequency (Ac.f), mineralized surface per bone surface (MS/BS) and osteoblast-(Ob.s/BS) and osteoclast surfaces (Oc.s/BS), as shown in Table 3. There was also a statistically significant correlation between osteoid thickness (O.Th) and fluoride activity at the anterior iliac crest ( $\text{FUR}_{\text{mean}}$ ). However, there was no correlation between  $K_i$  mean and  $\text{FUR}_{\text{mean}}$  and osteoid volume of bone volume (OV/BV) or mineralization lag time (Mlt). The correlation between fluoride activity and several histomorphometric and laboratory parameters is shown in Fig. 3.

#### 3.3.2. Correlation between $^{18}\text{F}$ -NaF PET and biochemical markers

$^{18}\text{F}$ -NaF PET measurements of  $K_i$  mean in the lumbar region and  $\text{FUR}_{\text{mean}}$  at the anterior iliac crest were also directly compared to biochemical markers such as PTH using the Spearman rank correlation test. There was a statistically significant correlation between PTH and

$K_i$  mean and  $\text{FUR}_{\text{mean}}$  levels, as shown in Table 3. There was no statistical correlation between  $K_i$  mean and  $\text{FUR}_{\text{mean}}$  and ionized calcium and alkaline phosphate. A weak correlation between phosphorus and  $K_i$  and  $\text{FUR}_{\text{mean}}$  was also observed, see Table 3.

There was some variability between fluoride uptake into bone between the lumbar spine and anterior iliac crest, however the correlation between  $K_i$  mean in the lumbar spine and  $\text{FUR}_{\text{mean}}$  at the iliac crest was good,  $R_s = 0.92$  and  $p < 0.001$ , see Table 3. Dialysis vintage or dialysis modality did not affect fluoride activity in the PET scan. Age affected the fluoride activity by lowering it, the correlation was stronger in the lumbar spine than in the anterior iliac crest. The healthy subjects fluoride activity in the lumbar region ( $K_i$  mean) was 0.039 (0.038–0.044) mL/min/mL and at the anterior iliac crest ( $\text{FUR}_{\text{mean}}$ ) 0.037 (0.032–0.044) mL/min/mL. The mean fluoride activity in the study group according to turnover is shown in Table 2, and images of PET/CT in Fig. 4.

#### 3.3.3. Diagnostic accuracy of $^{18}\text{F}$ -NaF PET for low turnover

In the  $^{18}\text{F}$ -NaF PET-scan, turnover was defined as low if  $^{18}\text{F}$ -activity was below the cut-off value (0.040 mL/min/mL) in the lumbar region or at the anterior iliac crest.  $^{18}\text{F}$ -NaF PET recognized 13 out of 17 patients with low turnover based on the bone biopsy. To test  $^{18}\text{F}$ -NaF PET imaging as a diagnostic tool when evaluating dialysis patients, we defined the ROC-curve after equalizing the study group for parametric measurements using a Natural-logarithm. In ROC analysis for discriminating low turnover from non-low turnover, when turnover was defined by BFR/BS and activation frequency, fluoride activity in the PET-scan had an AUC of 0.82. The sensitivity of  $^{18}\text{F}$ -NaF PET to distinguish between dialysis patients with low turnover from those with normal or high turnover was 76%, specificity 78%, positive predictive value 87% and negative predictive value 64%, see Table 4.

#### 3.3.4. Diagnostic accuracy of $^{18}\text{F}$ -NaF PET for high turnover

Because of the small amount of patient with high turnover ( $n = 3$ ), the ROC-curve could not be defined.  $^{18}\text{F}$ -NaF PET recognized all three patients with high turnover, but there were six false positives. Because of the small number of patients with high turnover, sensitivity and specificity of the method could not be calculated.

Diagnostic accuracy of PTH in this study population was poor. In ROC analysis for discriminating low turnover from non-low turnover, PTH had an AUC of 0.64. When cut-off of PTH was set at 200 ng/mL, sensitivity was 35% and specificity 78%, see Table 4.

## 4. Discussion

This study shows a strong correlation between fluoride activity in  $^{18}\text{F}$ -NaF PET imaging and histomorphometric parameters obtained by bone biopsy in dialysis patients. The strongest correlation was discovered between  $^{18}\text{F}$ -NaF PET and activation frequency, bone formation rate and osteoclast surfaces. This correlation was also significant between osteoblast surfaces, erosion surfaces and mineralized surfaces.  $^{18}\text{F}$ -NaF PET sensitivity to differentiate patients with low turnover from non-low based on these results was 76% and specificity 78% with an AUC of 0.82.  $^{18}\text{F}$ -NaF PET was superior to PTH to differentiate low turnover from non-low turnover.  $^{18}\text{F}$ -NaF PET recognized all patients with high turnover in the bone biopsy, but because of too few patients, sensitivity and specificity calculations could not be performed.

Bone biopsy is currently the gold standard for evaluation of CKD patients with ROD [1] and also the only method to assess the response to therapy. With bone biopsy, it is possible to get information about bone turnover, as well as mineralization and volume. However, bone biopsy is not easily reproducible and there is probably substantial intraindividual variability between patients [35]. In addition, bone biopsy gives information of only one site of the skeleton. This was highlighted in a study, where the microarchitecture of the iliac crest compared to the femoral neck and subtrochanteric femoral shaft using

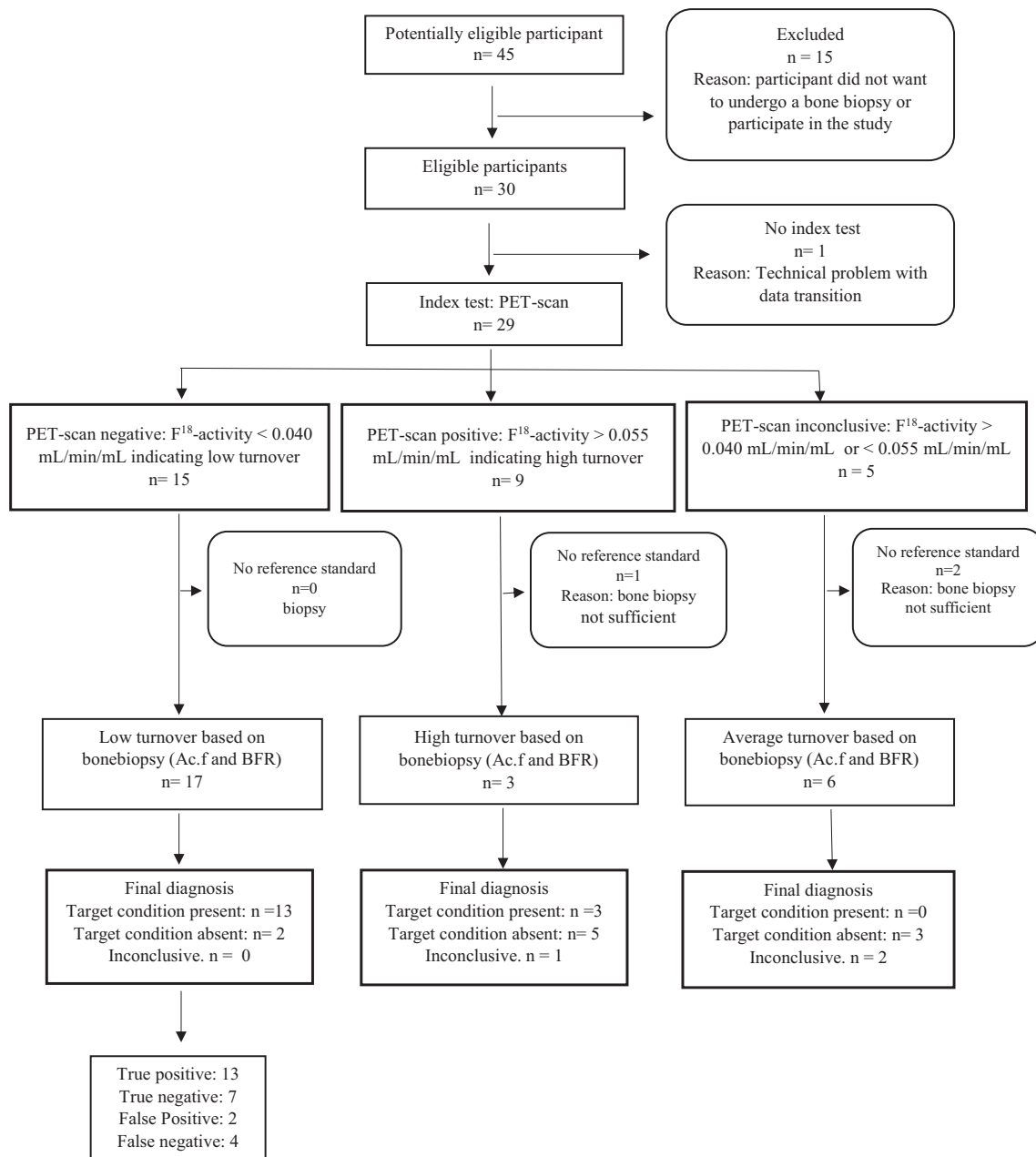


Fig. 2. Flow diagram of patients.

quantitative histomorphometry was assessed. It demonstrated significant heterogeneity in the microarchitecture of bone in different sites [36]. Bone biopsy can also cause procedural morbidity although severe complications are rare. Furthermore, the analysis requires time and highly skilled bone histomorphometrist. The interpretation of histomorphometric parameters and how to apply the analysis in clinical practice is not unambiguous.

Several noninvasive imaging methods have been investigated in CKD patients with mineral and bone disorder, such as DXA, high-resolution peripheral computed tomography (HR-pQCT) and magnetic resonance imaging. DXA is suitable for screening fracture risk in CKD-patients, but is not able to specify the underlying histopathology or to guide treatment [37]. HR-pQCT is a 3-dimensional imaging method, which can detect microarchitectural changes in trabecular and cortical bone and enables assessment of bone density and volume [21]. Magnetic resonance imaging quantify bone microarchitecture and in one small study, it showed association with indices from bone biopsy [38].

Still, these are static imaging methods.

<sup>18</sup>F-NaF PET may have some strengths over bone biopsy and other noninvasive methods, such as its noninvasiveness, speed, and readiness to produce reports. More importantly, it can give a more extensive picture of the whole skeleton. <sup>18</sup>F-NaF PET can be applied in a clinical setting and it is reproducible. No contrast agent is needed. On the other hand, PET-scans cause radiation. The radiation amount from the <sup>18</sup>F-NaF PET-scan is approximately 6 mSv which is about 50% of the radiation dose of a CT-scan of the abdomen. The radiation of DXA is approximately 0.01 mSv. PET-scan can also be considered effective, as the cost, at least in Finland, is less than the costs of a bone biopsy.

<sup>18</sup>F-fluoride seems to be a suitable tracer for measuring bone metabolism and is often used in clinical settings, for example when diagnosing bone metastasis in cancer patients [39]. It has earlier been shown in a smaller study by Messa et al., that <sup>18</sup>F-NaF PET correlates with bone histomorphometry [26], supporting our results. <sup>18</sup>F-NaF PET has also been proven suitable for evaluating response of teriparatide

**Table 2**  
Histomorphometric and imaging parameters according to turnover in dialysis patients.

	High turnover (n = 3)	Normal turnover (n = 6)	Low turnover (n = 17)	p-Value
BFR/BS ( $\mu\text{m}^3/\mu\text{m}^2/1$ day)	95.9 (93.0–107.6)	66.2 (52.6–83.8)	18.9 (14.3–30.3)	< 0.001
MAR ( $\mu\text{m}/\text{day}$ )	1.01 (0.99–1.02)	0.93 (0.7–1.2)	0.7 (0.6–0.9)	0.01
Oc.S/BS (%)	3.5 (1.4–6.7)	2.5 (1.1–4.4)	0.8 (0.001–1.6)	0.02
Ob.s/BS (%)	7.2 (3.2–16.9)	4.7 (2.5–14.9)	1.7 (0.1–3.2)	0.008
Mlt (d)	31.4 (22.3–34.8)	32.1 (23.7–38.9)	66.4 (34.0–99.8)	0.04
MS/BS (%)	9.5 (9.4–10.7)	6.6 (4.9–10.5)	2.7 (1.9–4.9)	0.002
O.th (Lm)	8.7 (7.2–10.0)	7.7 (5.9–10.7)	5.6 (4.9–6.6)	0.01
Ac.f/year	0.82 (0.67–0.83)	0.48 (0.46–0.56)	0.18 (0.13–0.28)	< 0.001
OS/BS (%)	38.4 (24.1–40.8)	25.5 (20.1–33.9)	23.2 (18.1–31.7)	0.26
ES/BS (%)	4.0 (2.4–6.9)	3.7 (2.4–4.4)	1.6 (0.5–2.9)	0.06
OV/BV (%)	6.8 (5.5–7.8)	3.4 (3.2–5.3)	3.1 (2.4–3.9)	0.03
BV/TV (%)	18.2 (18.1–25.9)	24.0 (16.9–27.3)	18.4 (13.1–24.4)	0.57
DXA BMD T-score (lumbar)	−1.1 (−2.3–0.2)	−1.65 (−2.65 to −0.7)	−0.6 (−2.28–0.45)	0.44
DXA BMD T-score (hip)	−2.4 (−2.6 to −1.6)	−2.05 (−2.675 to −1.88)	−2 (−3 to −0.95)	0.85
Mean Ki (L1–L4) mL/min/mL	0.067 (0.055–0.077)	0.052 (0.038–0.056)	0.038 (0.031–0.043)	0.02
Mean FUR (hip) mL/min/mL	0.065 (0.050–0.066)	0.055 (0.038–0.071)	0.038 (0.032–0.045)	0.01

**Table 3**  
Correlation between  $^{18}\text{F}$ -Sodium fluoride positron emission tomography and bone histomorphometry.

N = 26	$K_i$ mean (L1–L4)	FUR <sub>mean</sub> (iliac crest)
BFR/BS ( $\mu\text{m}^3/\mu\text{m}^2/1$ day)	$r_s = 0.63, p < 0.001$	$r_s = 0.66, p < 0.001$
ES/BS ( $\mu\text{m}/\text{day}$ )	$r_s = 0.57, p = 0.002$	$r_s = 0.60, p = 0.002$
Oc.S/BS (%)	$r_s = 0.62, p < 0.001$	$r_s = 0.62, p < 0.001$
Ob.S/BS (%)	$r_s = 0.49, p = 0.01$	$r_s = 0.58, p = 0.003$
MS/BS (%)	$r_s = 0.55, p = 0.003$	$r_s = 0.57, p = 0.003$
Ac.f/year	$r_s = 0.60, p = 0.002$	$r_s = 0.65, p < 0.001$
O.Th (Lm)	$p = 0.10$	$r_s = 0.48, p = 0.01$
OV/BV %	$p = 0.16$	$p = 0.10$
Mlt (d)	$p = 0.16$	$p = 0.25$
PTH ng/ml	$r_s = 0.55, p = 0.003$	$r_s = 0.58, p = 0.003$
Pi mmol/l	$r_s = 0.40, p = 0.04$	$r_s = 0.41, p = 0.04$
Ca-ion mmol/l	$p = 0.85$	$p = 0.85$
tALP U/l	$p = 0.30$	$p = 0.30$
FUR <sub>mean</sub> (iliac crest)	$R_s = 0.92, p < 0.001$	

BFR = bone formation rate, ES/BS = erosion surface per bone surface, Oc.S/BS = osteoclast surface, Ob.s/BS = osteoblast surface, MS/BS = mineralized surface/bone surface, Ac.f = activation frequency, O.th = osteoid thickness, OV/BV = osteoid volume of bone volume, Mlt = mineralization lag time. PTH = parathormone, Pi = phosphorus, ca-ion = ionized calcium ion, tALP = total alkaline phosphatase.  $K_i$  mean reflects the fluoride activity in the PET scan at the lumbar spine (L1–L4) and FUR<sub>mean</sub> the fluoride activity at the anterior iliac crest.  $p < 0.05$  is statistical significant.

treatment [29] and risedronate treatment [40] in patients with osteoporosis. Several studies have confirmed the differences in regional skeletal kinetics measured by  $^{18}\text{F}$ -NaF PET [24,41,42]. However, 25 years after the study of Messa et al. [26], PET-imaging techniques have evolved substantially, new indications for PET-imaging have been developed and especially availability has improved.  $^{18}\text{F}$ -NaF PET could be used in a clinical setting, for example to differentiate low turnover patients before starting osteoporosis medication, but as a supplement to other diagnostic tools in use. Further studies are under way to assess, how well the effect of treatment of renal osteodystrophy and osteoporosis can be assessed by PET-imaging in CKD patients.

PTH is widely used when evaluating and treating patients with ROD, but its predictive value to estimate underlying bone histology has been stated to be poor [18]. No biomarker in clinical use has yet been proven suitable or superior to PTH. In our study,  $^{18}\text{F}$ -NaF PET also correlated with PTH, which was somewhat surprising. This can partly be explained by the cross-sectional setting of our study. Another explanation can be the narrow range of PTH values in this study population, with only a few very low or high values. In our study PTH's diagnostic accuracy was inferior to the PET-scan.

There are several disconcerting factors to be taken into account,

when interpreting the PET results. Osteoporosis is known to lower the fluoride activity in the PET-scan compared to osteopenic and healthy subjects [28]. In our study population, 24% had osteoporosis based on the bone biopsy. All the patients with osteoporosis in the bone biopsy also had low turnover, of which  $^{18}\text{F}$ -NaF PET recognized 83%. Previous studies have also shown that age affects fluoride activity [43]. Age correlation was not corrected in the bone biopsies and therefore we did not perform age correction in the analyses of PET images either. This emphasizes the complexity of ROD and the challenge for evaluation of bone quality and quantity of dialysis patients, especially elderly patients with osteoporosis.

The limitations of our study are the relatively small number of studied patients and especially the few patients with high turnover. Due to this, multivariate analysis was not possible to perform. In most of the published studies of CKD-MBD, the definition of normal BFR has been between 1.8 and 3.8  $\text{mm}^3/\text{cm}^3/\text{y}$ . These reference values come from the highly cited work of Malluche's group [44]. The cut-off values of fluoride activity in the PET-scan were set accordingly. In our study, 65% had low turnover according to Malluche's definition of normal turnover [2], which is in line with previous studies [2,19]. However, it is possible that age distribution of our study population could have had an impact on the bone formation rate.

According to the prevailing practice at Turku PET-centre, also 7 healthy subjects underwent a PET-scan to confirm the feasibility of the PET-method. Their mean  $K_i$  (0,039 ml/min/ml) was comparable to the respective mean  $K_i$  (0,035 ml/min/ml) of normal postmenopausal (age 58.5 years) women [28]. The healthy subjects did not undergo a bone biopsy and were not matched to the study population. The  $K_i$  cut-off used in this study applies to this dialysis population, it is not a universal cut-off that can be applied to any disease, and it is not applicable to the healthy controls. Further research is needed to determine possible differences of the  $K_i$  cut-off in the PET scan in different CKD stages.

In conclusion, the result of our study highlights the possible future role of  $^{18}\text{F}$ -NaF PET as a noninvasive diagnostic tool in dialysis patients with renal osteodystrophy and low turnover bone disease. However, further research is needed to determine the PET method's possible role in clinical practice with a larger patient population.

Data is presented as median (interquartile range). BFR/BS = bone formation rate per bone surface, Oc.S/BS = osteoclast surface per bone surface, Ob.S/BS = osteoblast surface per bone surface, MAR = mineral apposition rate, Mlt = mineralization lag time, MS/BS = mineralized surface per bone surface, O.th = osteoid thickness, Ac.f = activation frequency per year, OS/BS = osteoid surface per bone surface, ES/BS = erosion surface per bone surface, OV/BV = osteoid volume of bone volume, BV/TV = bone volume of tissue volume. Mean Ki (L1–L4) reflects the fluoride activity in the PET scan in the lumbar spine and Mean FUR (hip) the fluoride activity at the

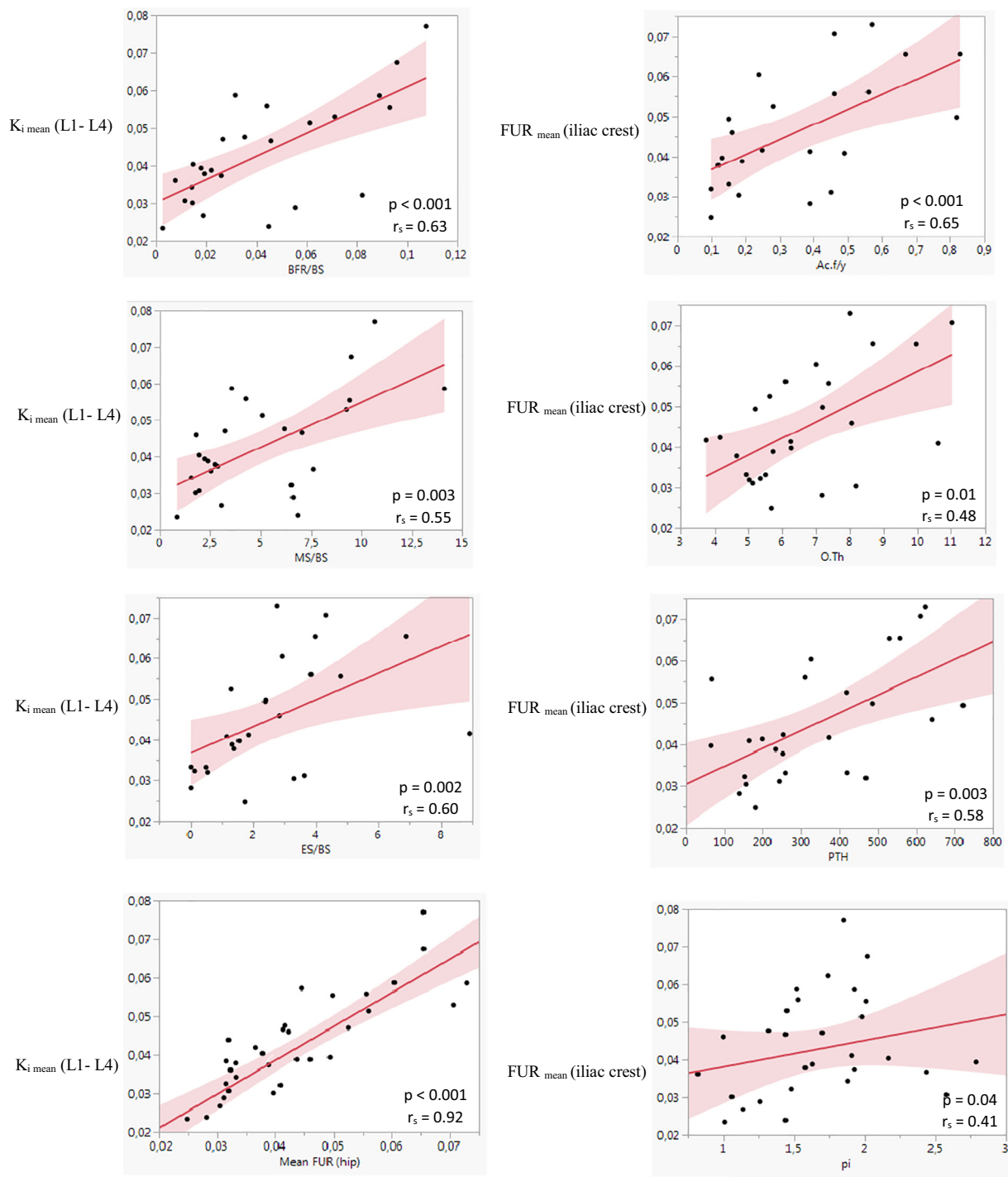


Fig. 3. Correlation between  $^{18}\text{F}$ -NaF PET and Histomorphometric Parameters.

anterior iliac crest.  $p < 0.05$  is statistically.

**Acknowledgements**

This trial has in part been presented in abstract form at the 55th ERA-EDTA Congress in Copenhagen 2018.

**Authors' contributions**

Research idea and study design: KM, NK, MS; data analysis/interpretation: LA, MS; statistical analysis: LA, EL; supervision or mentorship; HK, NK, KM. Each author contributed important intellectual

content during manuscript drafting or revision and accepts accountability for the overall work by ensuring that questions pertaining to the accuracy or integrity of any portion of the work are appropriately investigated and resolved.

**Funding**

Grants were received from the Finska Läkaresällskapet, Suomen Kulttuurirahaston Varsinais-Suomen rahasto and the Perklén Foundation, Helsinki, Finland.

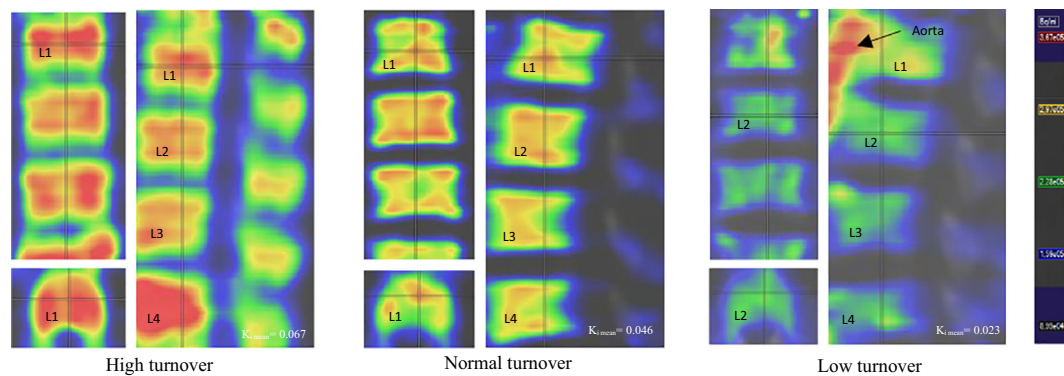


Fig. 4. Images of patients with high, normal and low turnover bone disease in the dynamic  $^{18}\text{F}$ -NaF PET scan of the lumbar spine.

Table 4

Diagnostic accuracy of  $^{18}\text{F}$ -NaF PET and PTH for identifying patients with.

Variables	AUC	Criterion	Sensitivity %	Specificity%	PPV %	NPV %
$^{18}\text{F}$ -Fluoride activity in the PET-scan	0.82	Cut-off 0.040 mL/min/mL	76%	78%	87%	64%
PTH	0.64	< 200 ng/ml	35%	78%	75%	39%

### Declaration of competing interest

The results presented in this paper have not been published previously in whole or part. All the authors declared no competing interests.

### References

- [1] Kidney Disease: Improving Global Outcomes (KDIGO) CKD-MBD Work Group, KDIGO clinical practice guideline for the diagnosis, evaluation, prevention, and treatment of Chronic Kidney Disease-Mineral and Bone Disorder (CKD-MBD), *Kidney Int. Suppl.* 113 (2009) S1–130 (doi:1).
- [2] H. Malluche, Renal osteodystrophy in the first decade of the new millennium: analysis of 630 bone biopsies in black and white patients, *J. Bone Miner. Res.* 26 (2011) 1368–1376.
- [3] H. Malluche, Differences in bone quality in low- and high-turnover renal osteodystrophy, *J. Am. Soc. Nephrol.* 23 (2012) 525–532.
- [4] H. Malluche, The importance of bone health in end-stage renal disease: out of the frying pan, into the fire? *Nephrol. Dial. Transplant.* 19 (Suppl. 1) (2004) 9–13.
- [5] H.H. Malluche, M.C. Monier-Faugere, Renal osteodystrophy: what's in a name? Presentation of a clinically useful new model to interpret bone histologic findings, *Clin. Nephrol.* 65 (2006) 235–242.
- [6] S.M. Sprague, The role of the bone biopsy in the diagnosis of renal osteodystrophy, *Semin. Dial.* 13 (2000) 152–155.
- [7] M.D. Danese, J. Kim, Q.V. Doan, M. Dylan, R. Griffiths, G.M. Chertow, PTH and the risks for hip, vertebral, and pelvic fractures among patients on dialysis, *Am. J. Kidney Dis.* 47 (2006) 149–156.
- [8] T.L. Nickolas, S. Cremers, A. Zhang, et al., Discriminants of prevalent fractures in chronic kidney disease, *J. Am. Soc. Nephrol.* 22 (2011) 1560–1572.
- [9] L. Robertson, C. Black, N. Fluck, et al., Hip fracture incidence and mortality in chronic kidney disease: the GLOMMS-II record linkage cohort study, *BMJ Open* 8 (2018) e20312.
- [10] J. Bover, P. Evenepoel, P. Ureña-Torres, et al., Pro: cardiovascular calcifications are clinically relevant, *Nephrol. Dial. Transplant.* 30 (2015) 345–351.
- [11] G. Coen, P. Ballanti, D. Mantella, et al., Bone turnover, osteopenia and vascular calcifications in hemodialysis patients. A histomorphometric and multislice CT study, *Am. J. Nephrol.* 29 (2009) 145–152.
- [12] D.V. Barreto, F. Barreto, C. Abd, et al., Association of changes in bone remodeling and coronary calcification in hemodialysis patients: a prospective study, *Am. J. Kidney Dis.* 52 (2008) 1139–1150.
- [13] P. Miller, The role of bone biopsy in patients with chronic renal failure, *Clin. J. Am. Soc. Nephrol.* 3 (Suppl. 3) (2008) 140–150.
- [14] S.M. Ott, Histomorphometric measurements of bone turnover, mineralization, and volume, *Clin. J. Am. Soc. Nephrol.* 3 (Suppl. 3) (2008) 151.
- [15] D.W. Dempster, J.E. Compston, M.K. Drezner, et al., Standardized nomenclature, symbols, and units for bone histomorphometry: a 2012 update of the report of the ASBMR Histomorphometry Nomenclature Committee, *J. Bone Miner. Res.* 28 (2013) 2–17.
- [16] J. Herberth, A.J. Branscum, H. Mawad, T. Cantor, M. Monier-Faugere, H.H. Malluche, Intact PTH combined with the PTH ratio for diagnosis of bone turnover in dialysis patients: a diagnostic test study, *Am. J. Kidney Dis.* 55 (2010) 897–906.
- [17] G. Lehmann, G. Stein, M. Hüller, R. Schemer, K. Ramakrishnan, W.G. Goodman, Specific measurement of PTH (1-84) in various forms of renal osteodystrophy (ROD) as assessed by bone histomorphometry, *Kidney Int.* 68 (2005) 1206–1214.
- [18] G. Garrett, S. Sardiwal, E.J. Lamb, D.J.A. Goldsmith, PTH—a particularly tricky hormone: why measure it at all in kidney patients? *Clin. J. Am. Soc. Nephrol.* 8 (2013) 299–312.
- [19] S.M. Sprague, E. Bellorin-Font, V. Jorgetti, et al., Diagnostic accuracy of bone turnover markers and bone histology in patients with CKD treated by dialysis, *Am. J. Kidney Dis.* 67 (2016) 559–566.
- [20] J. Herberth, M. Monier-Faugere, H.W. Mawad, et al., The five most commonly used intact parathyroid hormone assays are useful for screening but not for diagnosing bone turnover abnormalities in CKD-5 patients, *Clin. Nephrol.* 72 (2009) 5–14.
- [21] S. Salam, O. Gallagher, F. Gossiel, M. Paggioli, A. Khwaja, R. Eastell, Diagnostic accuracy of biomarkers and imaging for bone turnover in renal osteodystrophy, *J. Am. Soc. Nephrol.* 29 (2018) 1557–1565.
- [22] Y. Al-Beyatti, M. Siddique, M.L. Frost, I. Fogelman, G.M. Blake, Precision of  $^{18}\text{F}$ -fluoride PET skeletal kinetic studies in the assessment of bone metabolism, *Osteoporos. Int.* 23 (2012) 2535–2541.
- [23] E. Even-Sapir, E. Mishani, G. Flusser, U. Metzger,  $^{18}\text{F}$ -Fluoride positron emission tomography and positron emission tomography/computed tomography, *Semin. Nucl. Med.* 37 (2007) 462–469.
- [24] M.L. Frost, J.E. Compston, D. Goldsmith, et al., ( $^{18}\text{F}$ )-fluoride positron emission tomography measurements of regional bone formation in hemodialysis patients with suspected adynamic bone disease, *Calcif. Tissue Int.* 93 (2013) 436–447.
- [25] G.M. Blake, S.J. Park-Holohan, G.J. Cook, I. Fogelman, Quantitative studies of bone with the use of  $^{18}\text{F}$ -fluoride and  $^{99\text{m}}\text{Tc}$ -methylene diphosphonate, *Semin. Nucl. Med.* 31 (2001) 28–49.
- [26] C. Messa, W.G. Goodman, C.K. Hoh, et al., Bone metabolic activity measured with positron emission tomography and [ $^{18}\text{F}$ ]fluoride ion in renal osteodystrophy: correlation with bone histomorphometry, *J. Clin. Endocrinol. Metab.* 77 (1993) 949–955.
- [27] G.J.R. Cook, G.M. Blake, P.K. Marsden, B. Cronin, I. Fogelman, Quantification of skeletal kinetic indices in Paget's disease using dynamic  $^{18}\text{F}$ -fluoride positron emission tomography, *J. Bone Miner. Res.* 17 (2002) 854–859.
- [28] M.L. Frost, I. Fogelman, G.M. Blake, P.K. Marsden, G. Cook, Dissociation between global markers of bone formation and direct measurement of spinal bone formation in osteoporosis, *J. Bone Miner. Res.* 19 (2004) 1797–1804.
- [29] M.L. Frost, M. Siddique, G.M. Blake, et al., Differential effects of teriparatide on regional bone formation using ( $^{18}\text{F}$ )-fluoride positron emission tomography, *J. Bone Miner. Res.* 26 (2011) 1002–1011.
- [30] S. Moe, T. Drüeke, J. Cunningham, et al., Definition, evaluation, and classification of renal osteodystrophy: a position statement from Kidney Disease: Improving Global Outcomes (KDIGO), *Kidney Int.* 69 (2006) 1945–1953.
- [31] G.J. Cook, M.A. Lodge, P.K. Marsden, A. Dynes, I. Fogelman, Non-invasive assessment of skeletal kinetics using fluorine-18 fluoride positron emission tomography: evaluation of image and population-derived arterial input functions, *Eur. J. Nucl. Med.* 26 (1999) 1424–1429.
- [32] T. Puri, G.M. Blake, M.L. Frost, et al., Validation of image-derived arterial input functions at the femoral artery using  $^{18}\text{F}$ -fluoride positron emission tomography, *Nucl. Med. Commun.* 32 (2011) 808–817.
- [33] M. Siddique, M.L. Frost, G.M. Blake, et al., The precision and sensitivity of ( $^{18}\text{F}$ )-fluoride PET for measuring regional bone metabolism: a comparison of quantification methods, *J. Nucl. Med.* 52 (2011) 1748–1755.
- [34] J.A. Thie, Clarification of a fractional uptake concept, *J. Nucl. Med.* 36 (1995) 711–712.



- [35] P. Evenepoel, G.J.S. Behets, M.R. Laurent, P.C. D'Haese, Update on the role of bone biopsy in the management of patients with CKD-MBD, *J. Nephrol.* 30 (2017) 645–652.
- [36] X. Tong, I.S. Burton, J.S. Jurvelin, H. Isaksson, H. Kroger, Iliac crest histomorphometry and skeletal heterogeneity in men, *Bone Rep.* 6 (2016) 9–16.
- [37] Anonymous Erratum: Kidney Disease: Improving Global Outcomes (KDIGO) CKD-MBD Update Work Group, KDIGO 2017 clinical practice guideline update for the diagnosis, evaluation, prevention, and treatment of Chronic Kidney Disease-Mineral and Bone Disorder (CKD-MBD), *Kidney Int Suppl.* 2017;7:1-59, *Kidney Int. Suppl.* 2017 (7) (2011) e1.
- [38] A.K. Sharma, N.D. Toussaint, G.J. Elder, et al., Magnetic resonance imaging based assessment of bone microstructure as a non-invasive alternative to histomorphometry in patients with chronic kidney disease, *Bone* 114 (2018) 14–21.
- [39] M. Araz, G. Aras, O.N. Kucuk, The role of  $^{18}\text{F}$ -NaF PET/CT in metastatic bone disease, *J. Bone Oncol.* 4 (2015) 92–97.
- [40] M.L. Frost, G.J.R. Cook, G.M. Blake, P.K. Marsden, N.A. Benatar, I. Fogelman, A prospective study of risedronate on regional bone metabolism and blood flow at the lumbar spine measured by  $^{18}\text{F}$ -fluoride positron emission tomography, *J. Bone Miner. Res.* 18 (2003) 2215–2222.
- [41] C. Schiepers, J. Nuyts, G. Bormans, et al., Fluoride kinetics of the axial skeleton measured in vivo with fluorine-18-fluoride PET, *J. Nucl. Med.* 38 (1997) 1970–1976.
- [42] G.J. Cook, M.A. Lodge, G.M. Blake, P.K. Marsden, I. Fogelman, Differences in skeletal kinetics between vertebral and humeral bone measured by  $^{18}\text{F}$ -fluoride positron emission tomography in postmenopausal women, *J. Bone Miner. Res.* 15 (2000) 763–769.
- [43] T. Derlin, T. Janssen, J. Salamon, et al., Age-related differences in the activity of arterial mineral deposition and regional bone metabolism: a  $^{18}\text{F}$ -sodium fluoride positron emission tomography study, *Osteoporos. Int.* 26 (2015) 199–207.
- [44] H.H. Malluche, W. Meyer, D. Sherman, S.G. Massry, Quantitative bone histology in 84 normal American subjects. Micromorphometric analysis and evaluation of variance in iliac bone, *Calcif. Tissue Int.* 34 (1982) 449–455.